BRUKER LECTURE. The Nuclear Zeeman Interaction in Electron Resonance

N. M. Atherton

Department of Chemistry, The University of Sheffield, Sheffield S3 7HF, U.K.

1 Introduction

Elementary accounts of electron paramagnetic resonance (EPR) emphasize the hyperfine splitting in the spectra and explain how it arises and how it may be interpreted. This is quite proper for the hyperfine splitting often yields useful information very directly and in a fairly unsophisticated way. The analysis of spectra to extract hyperfine coupling constants can often be done under the assumption that the $\Delta M_S = 1, \Delta M_I = 0$ selection rule is valid. This selection rule implies that the transitions can be described using an energy level diagram which takes no account of the nuclear Zeeman energy and this in turn implies that the levels themselves are the eigenvalues of a Hamiltonian which does not contain the nuclear Zeeman interaction.

The $\Delta M_S = 1$, $\Delta M_I = 0$ selection rule provides an adequate basis for analysing the spectra of species in solutions and in some solids. However, it has been known for many years that it can be inappropriate for solids, where the dipolar component of the hyperfine interaction contributes to the hyperfine splitting, and that this condition occurs when the hyperfine interaction is comparable to the nuclear Zeeman energy. The effect was first observed and understood by McConnell,[1] Whiffen,[2] and Gordy[3] and their collaborators for radicals of general structure RR'CH which, at the time, were of especial interest as models of the aromatic CH fragment. Apart from practitioners of solid state ENDOR and ESEEM most practitioners of EPR have been able to get along very nicely without troubling about the matter and it has not featured prominently in the literature for some years. However, recent technological developments have made it possible to measure spectra at much higher fields than those traditionally used, for example at fields of 3.4, 5.4, and 8.9 T, corresponding to electron Larmor frequencies of 95,[4] 150,[5] and 250 GHz[6] respectively for $g = 2$. Since increasing the magnetic field increases the nuclear Zeeman energy while leaving the hyperfine interaction unchanged it seems possible that in high field experiments one may run into regimes where the two interactions become comparable and where the behaviour of the system in electron resonance experiments may be quite different from that which is observed at, say, X-band. In view of these considerations it appears timely to review the role of the nuclear Zeeman interaction in electron resonance.

It may be a comfort to those who are not familiar with these

matters if we emphasize at this point we will be dealing with solids, or situations where the rotational correlation is long, and that for any effect to show there must be considerable anisotropy in the hyperfine interaction.

2 Theoretical Considerations

In order to illustrate the points which we wish to emphasize it will be sufficient for us to consider an $S = \frac{1}{2}$ system described by the spin Hamiltonian

$$H = \mu_B B.g.S + S.A.I - \gamma B.I \tag{1}$$

where the three terms describe respectively the electron Zeeman, hyperfine, and nuclear Zeeman interactions. For full generality we should add a term describing the nuclear quadrupole interaction but the important physical points are best perceived if it is omitted.

We now assume that the electron Zeeman interaction is by far the largest term. This means that we neglect the field due to the nucleus at the electron and take the electron spin to be quantized in a field determined by the applied field as transformed by the operation of the g-tensor. The quality of this assumption improves with increasing strength of the applied field. We will comment on the effect of the anisotropy of the g-tensor later but for the moment take it to be isotropic. Now the electron spin can be taken to be quantized along the applied field and (1) becomes

$$H = \mu_B g B_0 M_S + (M_S I.A - \gamma B_0 I).I \tag{2}$$

where $M_S = +\frac{1}{2}$ and I is a unit vector defining the orientation of the applied field B_0 in the axis system in which A is expressed. The eigenvalues of this Hamiltonian are

$$E = g\mu_B B_0 M_S + \{M_S^2 I.A.A.I + \gamma^2 B_0^2 - 2M_S \gamma B_0 I.A.I\}^{\frac{1}{2}} M_I \tag{3}$$

which gives rather cumbersome expressions for the energies of the $\Delta M_S = 1$ EPR transitions but a rather more elegant one for the squares of the $\Delta M_I = 1$ ENDOR frequencies.

These results are obtained quite readily by making a judicious choice of the quantization axis for the nuclear spin, and this point is implicit or explicit in all the literature treatments.[1] [3,7,8] It is not necessary to rehearse the argument here but the important point to be realized is that the orientation of this axis depends on the electron spin state. The physical basis of this is clear when one considers the magnetic fields at the nucleus, as illustrated in Figures 1a, b. The total field at the nucleus, B_I, is the resultant of the applied field B_0 and the hyperfine field B_S which is itself, in general, compounded of an isotropic component parallel to B_0 and a dipolar part. Figures 1a and 1b may be taken to represent the $M_S = -\frac{1}{2}$ and $M_S = +\frac{1}{2}$ states respectively. It is clear that both the magnitude and orientation of B_I are dependent on the electron spin state when the hyperfine interaction is anisotropic.

It follows from all this that one must be careful with the nuclear spin eigenfunctions. For consistent calculations one needs them expressed in the same basis for the two electron spin states. For example if we chose the set $|M_S^-\rangle$, i.e. the eigenfunctions of I_Z for $M_S = -\frac{1}{2}$, as the basis then the eigenfunctions for $M_S = +\frac{1}{2}$ are linear combinations of these with admixture coefficients which depend on ϕ, the angle between B_I^- and B_I^+, Figure 1c. For $I = \frac{1}{2}$ one finds

Neil Atherton was brought up in Redcar, where he attended Sir William Turner's School, and was a student of the University of Birmingham. He has been active in the field of electron spin resonance and its applications since he began Ph.D. research under the supervision of Professor D. H. Whiffen in 1956. After a postdoctoral year with Professor S. I. Weissman at Washington University, St. Louis, he went to the University of Sheffield as an ICI Fellow in 1960 and eventually became Professor of Physical Chemistry there in 1975. He is currently Dean of the Faculty of Pure Science at Sheffield.

c
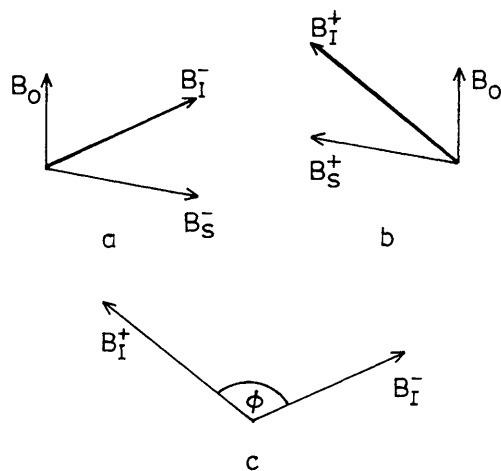
Figure 1 (a), (b) Magnetic fields experienced by a nucleus having an anisotropic hyperfine interaction with an electron spin, $S = \frac{1}{2}$ The applied field B_0 and the hyperfine field B_S combine to give a resultant B_I which provides the quantization axis for the nuclear spin For the two electron spin states the B_S vectors have the same magnitude but are antiparallel so the resultants B_I are different in both magnitude and orientation for them (c) Definition of the angle ϕ between the axes of quantization of the nuclear spin for the two electron spin states

$$|M_I^+ = +\tfrac{1}{2}\rangle = \cos(\phi/2)|M_I = +\tfrac{1}{2}\rangle + \sin(\phi/2)|M_I = -\tfrac{1}{2}\rangle \quad (4)$$

with the second function determined by the orthogonality requirement and where

$$\cos\phi = \frac{\gamma^2 B_0^2 - (1/4)(I\,A\,A\,I)}{[\{(1/4)(I\,A\,A\,I) + \gamma^2 B_0^2\}^2 - \gamma^2 B_0^2(I\,A\,A\,I)2]^{1/2}} \quad (5)$$

One may readily verify that when the hyperfine coupling is isotropic, or when B_0 lies along a principal value of the hyperfine coupling, then B_S and B_0 are collinear for both electron spin states, $\phi = 0$ or π Further, when B_S and B_0 are identical in length, B_I^+ and B_I^- are orthogonal so that $\cos(\phi/2) = \sin(\phi/2) = 2^{-\frac{1}{2}}$

These are the main points we need for the discussion which follows However, before proceeding it is convenient to tidy up the effect of g-anisotropy When there is g-anisotropy the electron is quantized along an axis which is not collinear with B_0, and the orientation of the field B_S at the nucleus reflects this misalignment The result is that g enters into all the expressions for the eigenvalues and eigenfunctions, where, for example, $I\,A$ is replaced by $I g\,A/(I g\,g\,I)^{\frac{1}{2}}$ However, the essential physical point is not changed the axis of quantization of the nuclear spin depends, in general, on the electron spin state

3 EPR Absorption Spectra

The disposition of the local fields at a nucleus depicted in Figure 1a is switched into that of Figure 1b when an EPR absorption occurs The nuclear spin state after the transition will be either $M_I^+ = +\frac{1}{2}$ or $M_I^+ = -\frac{1}{2}$ with relative probabilities determined by ϕ If $I = \frac{1}{2}$ there are now two observable transitions for each initial nuclear spin state From equation 4 we can see that the transition moments are $\sin(\phi/2)$ and $\cos(\phi/2)$ so that the intensities of the two transitions are $(\frac{1}{2})(1 \pm \cos\phi)$ It may be discerned from equation 5 that the two transitions have equal intensity when the nuclear Zeeman energy is equal to one half of the effective hyperfine interaction, $(I\,A\,A\,I)^{\frac{1}{2}}$ Further, the intensity-weighted mean position of the two transitions is equal to one half of the effective hyperfine interaction It is clearly wrong-headed to speak of these transitions as being 'allowed' or 'forbidden' we will refer to them as (M_I, M_I') transitions which may be strong or weak

The stick spectra depicted in Figure 2 exemplify the sort of behaviour just described They are calculated for the α-proton of
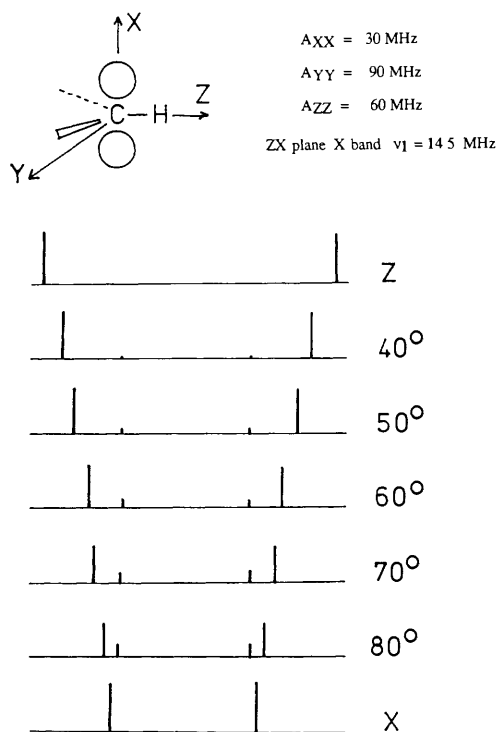
Figure 2 Orientation-dependence of the EPR spectrum for an α-proton at X-band

a C–H fragment at X-band ($\nu_I = 14\,5$ MHz) for the field exploring the plane containing the axis of the singly occupied $2p$ orbital (X) and the C–H bond (Z) It was assumed that $A_{XX} = -60$ MHz, $A_{ZZ} = -30$ MHz, values which have long been accepted as typical for the C–H fragment [9][8] When the field is close to X the hyperfine coupling is relatively large and to all intents and purposes the $\Delta M_I = 0$ selection rule applies However as the field approaches Z weak (M_I, M_I') transitions begin to show appreciable intensity although the spectrum becomes simple again when it lies along Z Figure 3 shows the development of the spectrum for the field lying 50° from Z as a function of increasing field corresponding to electron Larmor
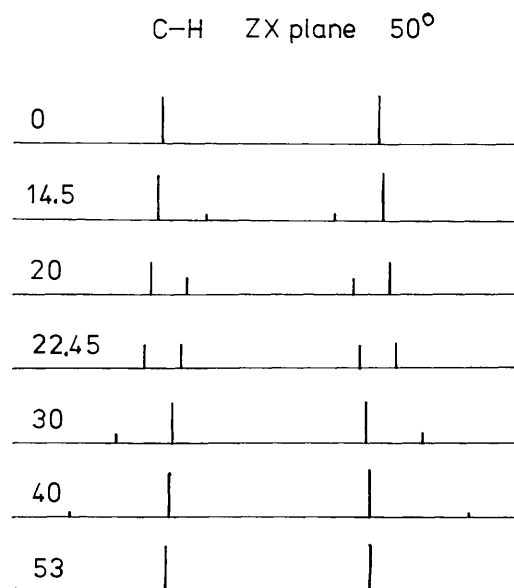
Figure 3 Field-dependence of the EPR spectrum for an α proton The figures indicate the value of ν_I/MHz 14 5 MHz corresponds to X band 53 MHz to Q-band When $\nu_I = 22\,45$ MHz $\phi = \pi\,2$

frequencies in the range X-band to Q-band This covers the field at which the nuclear Zeeman energy is half the effective hyperfine interaction We note that at the highest field the weak outer transitions have become 'proton spin flip' transitions their separation approaches a limiting value of $2\nu_I$ [10] [8]

All this is familiar for protons and it is clear that for them going to high fields causes no complications, especially as virtually all of the protons in systems of interest have smaller couplings than the one in the C—H fragment so that the nuclear Zeeman interaction dominates to determine the axis of quantization However, this will not be so for other nuclei, essentially all of which have smaller magnetogyric ratios As an $I = \frac{1}{2}$ example we consider ^{15}N this is not unrealistic for there can be merit in using isotopically substituted nitroxides as probes Figure 4 shows the appearance of the spectra at several frequencies They were calculated assuming that the field lies 70° from a principal hyperfine coupling of 129 MHz in a plane containing a second principal coupling of 24 55 MHz, these values having been scaled from those typical of the ^{14}N couplings in nitroxides
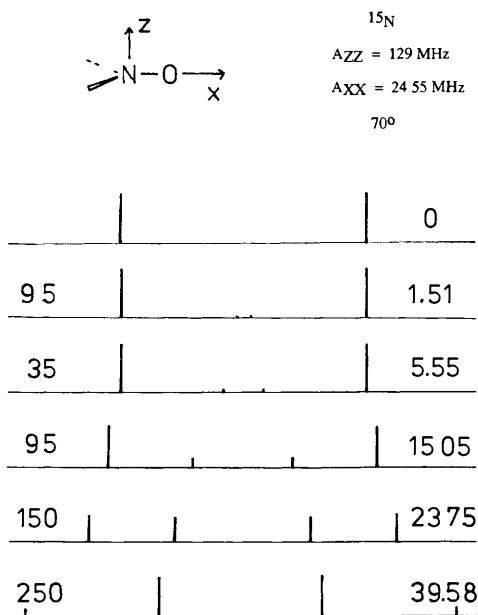

Figure 4 Field-dependence of the EPR spectrum of an ^{15}N-labelled nitroxide The figures on the left indicate ν_S/GHz, those on the right ν_I/MHz

Of course, nitroxides containing ^{14}N are of crucial interest Figure 5 indicates spectra calculated for the same orientation of the field as that defined above for the ^{15}N isotopomer for the fields used in recent EPR experiments [4] [6] The relevant principal values of the hyperfine tensor were taken to be 92 and 17 5 MHz It is interesting to note that at an EPR frequency of 150 GHz, where for this orientation the critical condition on the relative values of the effective hyperfine coupling and the nuclear Zeeman energy is close to being met, the intensity of the '$M_I = 0$' hyperfine component is very small The intensity would be exactly zero if the condition were exactly met $\phi = \pi/2$, the reason being that the nuclear spin is oriented perpendicular to the quantization axis for the $M_I = 0$ nuclear spin state and there is zero probability of it finding the equivalent orientation when the quantization axis is flipped by $\pi/2$

It is not difficult to identify other nuclei, quite familiar in X- and Q-band EPR, whose Zeeman energies are considerable at the highest fields at which EPR experiments have now been done It would seem prudent to consider whether this is significant in any experiment being carried out at high fields For example, the detailed shapes of powder spectra should reflect the occurrence of any transitions which are 'forbidden' at low field Again, when the principal axes of the g- and A-tensors are not
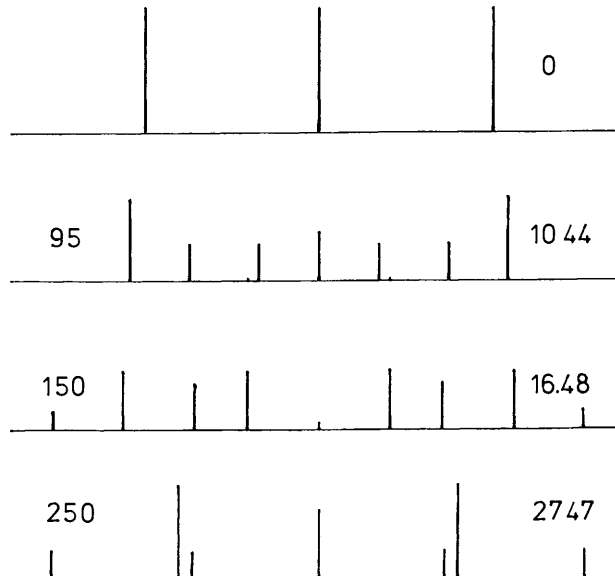

Figure 5 Field-dependence of the EPR spectrum of an ^{14}N-nitroxide, $A_{ZZ} = 92$ MHz, $A_{XX} = 17$ 5 MHz, same orientation as in Figure 4 The figures on the left indicate ν_S/GHz, those on the right ν_I/MHz

collinear then hyperfine features appearing at a g-extremum in a powder spectrum, which may well stand out very clearly at high field, may not simply reflect the effective hyperfine splitting

4 Electron Spin Echo Envelope Modulation (ESEEM)

The occurrence of (M_I, M_I') transitions is the cause of ESEEM The experiment was conceived, implemented, and analysed by Mims some 20 years ago,[11] but several years were to pass before it came into widespread use

The origin of the modulation of the echo observed following a 2-pulse $(\pi/2 - \tau - \pi)$ sequence can be understood from Figure 6 Here we show the evolution, in the rotating frame, of an $S = \frac{1}{2}$, $I = \frac{1}{2}$ system whose EPR spectrum comprises four (M_I, M_I') transitions In this figure the time evolution is to be read from the top and, instead of the dephasing and rephasing of the coherences being depicted in the conventional manner showing their
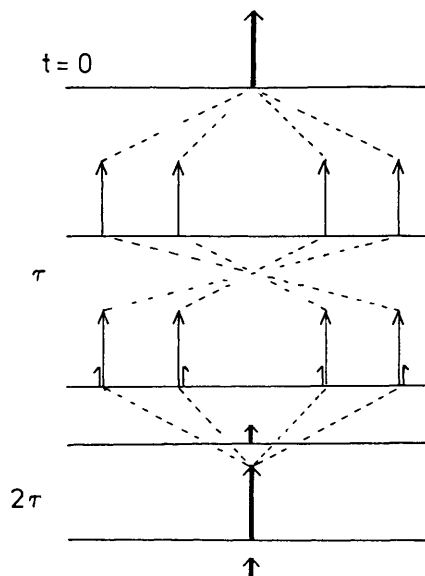

Figure 6 The formation of a modulated echo in a $(\pi/2 \quad \tau \quad \pi)$ pulsed experiment on an $S = \frac{1}{2}$, $I = \frac{1}{2}$ system whose EPR spectrum comprises (M_I, M_I') transitions See text for a detailed explanation

movement on a circle, we use a linear representation so that the horizontal axes in the diagrams represent angle The top diagram depicts the magnetization lying along ι after its rotation from z by the $\pi/2$ pulse along x The system is then allowed to evolve and the four coherences corresponding to the four (M_I, M_I') transitions fan out at rates determined by their Larmor frequencies until the π pulse, assumed to be applied along y, is applied at time τ This pulse has two effects The first, the normal one in echo experiments, is to rotate coherences about y by π The second effect, which is the crucial one for ESEEM, is that it creates new coherences which are in the 'wrong' place, that is, their angular displacement from ι is not that which they would have achieved had they moved at their Larmor frequencies during the interval τ These new coherences are indicated by the short arrows in the third diagram Further evolution of the system now takes all the coherences back towards the origin, y, but they do not all refocus simultaneously at time 2τ the new coherences arising from the second pulse arrive back earlier or later and the echo envelope is modulated It is clear that the modulation depends on the occurrence of the (M_I, M_I') transitions if the $\Delta M_S = 1, \Delta M_I = 0$ selection rule applied, so that the spectrum consisted of just two transitions, then all the spins would refocus simultaneously

The experiment was analysed by Mims,[11] his result for the form of the echo modulation function can be written[8]

$$v(\tau) \sim M_+^4 + M^4 + 2M_+^2 M^2 \{\cos \omega_{12}\tau + \cos \omega_{34}\tau\} - M_+^2 M^2 \{\cos \omega_{\tau+\tau} + \cos \omega \ \tau\} \quad (6)$$

where M_+ and M_- are the transition moments for the two (M_I, M_I') transitions, ω_{12} and ω_{34} are the two ENDOR frequencies, and ω_+ and ω_- are their sum and difference Recalling that the squares of the transition moments sum to unity we see immediately that the depth of modulation at the ENDOR frequencies should be a maximum when the two transition moments are equal, i e when the nuclear Zeeman energy is half the effective hyperfine interaction There is thus an optimum field for ESEEM measurements This conclusion is also reached from analysis of the 3-pulse ESEEM experiment in which the stimulated echo is detected[11]

The important use of ESEEM is to complement ENDOR in the measurement of small hyperfine interactions, such as those which obtain for ligand nuclei in transition metal complexes Taking ^{14}N as an example, X-band is clearly a good frequency to use for couplings of the order of 1 MHz since v_I is also 1 MHz However, for other nuclei with comparable hyperfine interactions but with larger magnetogyric ratios there may well be no advantage in going to high field and for studying small hyperfine couplings to ^{1}H and ^{19}F it may very often be advantageous to make ESEEM measurements at lower frequencies than X-band

5 Coherence Spectroscopy (COSY)

Two-dimensional (2D) magnetic resonance experiments were conceived by Jeener[12] and have become established as an indispensable part of NMR spectroscopy [13] Their development for EPR lagged behind that for NMR on account of the more demanding technology required to cope with the much shorter characteristic timescales, but notable progress has been made in the last few years In particular, Freed and his collaborators have implemented and analysed the EPR analogues of several established NMR experiments,[14] while a review by Schweiger gives a comprehensive overview of developments up to 1991 [15]

The NMR COSY experiment is a valuable way of unravelling the couplings in complex spin systems [16] The experiment comprises two $\pi/2$ pulses separated by an interval t_1 and the free induction decay is detected over the time regime t_2 following the second pulse Fourier transformation with respect to the time regimes t_1 and t_2 yields the 2D spectrum, in which the appearance of off-diagonal or cross peaks indicates coupling between pairs of spins In the absence of strong relaxation processes the COSY spectrum of an $S = \frac{1}{2}$ system in which there is hyperfine

coupling to a single nucleus, and in which the $\Delta M_S = 1, \Delta M_I = 0$ selection rule holds, is not expected to show cross peaks this has been confirmed by Gorcester and Freed[14][17] for a nitroxide in solution However, if the EPR spectrum comprises (M_I, M_I') transitions then cross peaks should be observed up to the time of writing, this experiment does not appear to have been implemented

6 Magnetization Transfer Experiments

Dynamical processes transfer magnetization from one part of a spectrum to another Chemical exchange is a transparent example but here we will concentrate on the transfer effected by slow rotational diffusion for a great deal of attention has been paid to devising and analysing EPR experiments to study and characterize such motion We will list three classes of experiment and comment on the implications for them of the occurrence of (M_I, M_I') transitions

An approach which is very direct and conceptually straightforward is the frequency-swept ELDOR experiment of Hyde et al [18] The principle may be understood by reference to Figure 7, which depicts very schematically the rigid lattice limit powder spectrum of a nitroxide radical having assumedly uniaxial anisotropic magnetic interactions The spectrum is pumped at a point corresponding to a particular orientation for, say, the $M_I = -1$ hyperfine component, for example at ω_p, and the response at another point, for example ω_o, is monitored The strength of that response is determined by the effectiveness at which saturation is induced at ω_p, and thus by T_1, and then the competition between spin–lattice relaxation and the rate at which slow rotational diffusion transfers the saturation to the observing point Data are collected by varying the separation between ω_p and ω_o and so this CW experiment is very time-consuming A great improvement in this respect can be obtained if a pulsed technique is used and it should be possible to do this using an experiment implemented by Freed and his group [14] Generically the experiment belongs to the class of 2D experiments which were introduced by Jeener et al for the study of chemical exchange,[19] and which are known as EXSY (from exchange spectroscopy), but which Freed very appropriately refers to as 2D-ELDOR The method has been used to study freely tumbling nitroxides and the potential for studying slow motion has been appreciated[14] but the experiment does not yet seem to have been implemented for the slow motional regime It is interesting to note in passing that this pair of experiments,
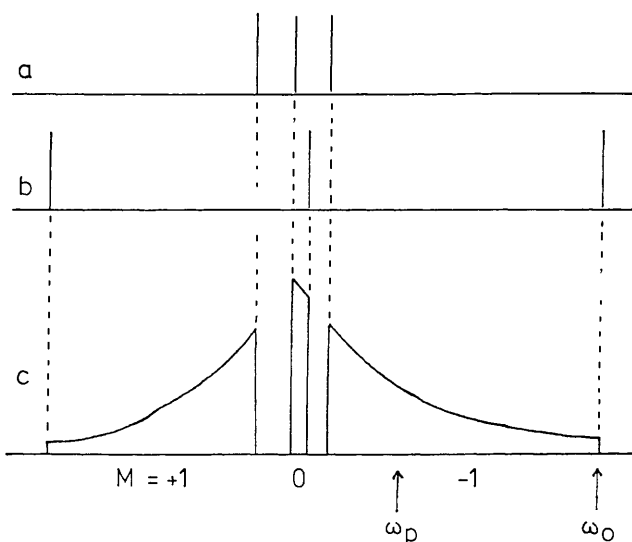
Figure 7 The construction of the powder EPR spectrum for a hypothetical uniaxial nitroxide The spectra for the perpendicular and parallel orientations are indicated at (a) and (b) respectively, the idealized powder absorption spectrum at (c)

frequency-swept ELDOR and 2D-ELDOR, form a very pleas-
ing illustration of the complementarity of double resonance and
2D experiments The third type of experiment we wish to
mention is saturation transfer EPR (ST-EPR) [20] Here one
detects, typically, the out-of-phase absorption at the second
harmonic of the modulation frequency, the sampling of different
parts of the spectrum being achieved because the field is modu-
lated This is a CW method and so is very widely available
although it needs to be handled with care [21]

In all of these experiments the nature of the response depends
on the transition moments of the transitions being excited The
transition rate depends on the transition moment in exactly the
same way irrespective of whether the oscillating field driving the
transition derives from coherent radiation or from stochastically
fluctuating magnetic interactions, and it follows that the spin–
lattice relaxation time is longer for a weak (M_I, M_I') transition
than it is for a strong one It is clear from Figures 4 and 5 that the
rigid lattice limiting spectra of nitroxides at high fields must
contain contributions from (M_I, M_I') transitions and so one
might expect to see manifestation of their occurrence through
comparison of magnetization transfer experiments performed at
different frequencies The point has been appreciated in respect
of ST-EPR[5] but it would appear that there is considerable scope
for further study of the matter

7 ENDOR Transition Moments

The core of this essay has been the fact that the orientation and
magnitude of the field experienced by a nucleus depends on the
electron spin state and the orientation of the applied field with
respect to the hyperfine tensor We move towards a conclusion
by considering the consequences for ENDOR transition
moments

In the usual experimental arrangement for ENDOR the r f
field is delivered by a coil whose axis is perpendicular to the
applied field, B_0, so that the r f field oscillates in a plane
perpendicular to B_0 In general this plane will not be perpendicu-
lar to the axis of quantization of the nuclear spin If the angle
between the r f field and the quantization axis is ψ then the
transition moment contains a factor $\sin \psi$ and the r f -induced
nuclear transition probability lies in the range $1 \geqslant \sin^2 \psi \geqslant 0$ It
follows that when the hyperfine and nuclear Zeeman energies are
comparable the intensities of ENDOR transitions can be
strongly orientation-dependent This effect, which will be fami-
liar to anyone who has made ENDOR measurements on single
crystals has been recognized and understood for many years [22]

Consideration of this matter has not figured prominently in
analyses of the results of orientation-selected ENDOR experi-
ments whereby one seeks information about anisotropic hyper-
fine interactions from powder samples The method, which was
initially developed by Hoffman, Kreilick, and Yordanov, and
their collaborators,[23] following up earlier work by Rist and
Hyde,[24] is now firmly established [25] The principles can be
understood by considering the idealized case of a uniaxial ligand
hyperfine coupling in a complex with a uniaxial g-tensor
Vanadyl complexes may approach this ideal limit and we use one
as an example in Figure 8 The EPR spectrum of a vanadyl
complex is shown in Figure 8a it is a typical example The ESR
absorption at point B, the low field extremum, arises from those
complexes in the $M_I = -7/2$ nuclear spin state for which B_0 lies
along g and the ENDOR response at that point arises from
those complexes only If the angle between the axes of g and A is
α then the ENDOR response is crystal-like, for in all the
complexes contributing to the response B_0 is inclined at α to the
axis of the hyperfine coupling, cf Figure 8b Such a response is
shown in Figure 8d, which is the high frequency [133]Cs ENDOR
signal observed from vanadyl-doped CsCl (the low frequency
component occurs close to zero frequency) If the field is set to
point B_θ of the EPR spectrum, the ENDOR response is from
complexes in which the field is inclined at θ to g but now, as can
be seen from Figure 8c this covers a range of orientations, from
$(\theta + \alpha)$ to $(\theta - \alpha)$, of the field with respect to A We thus expect a
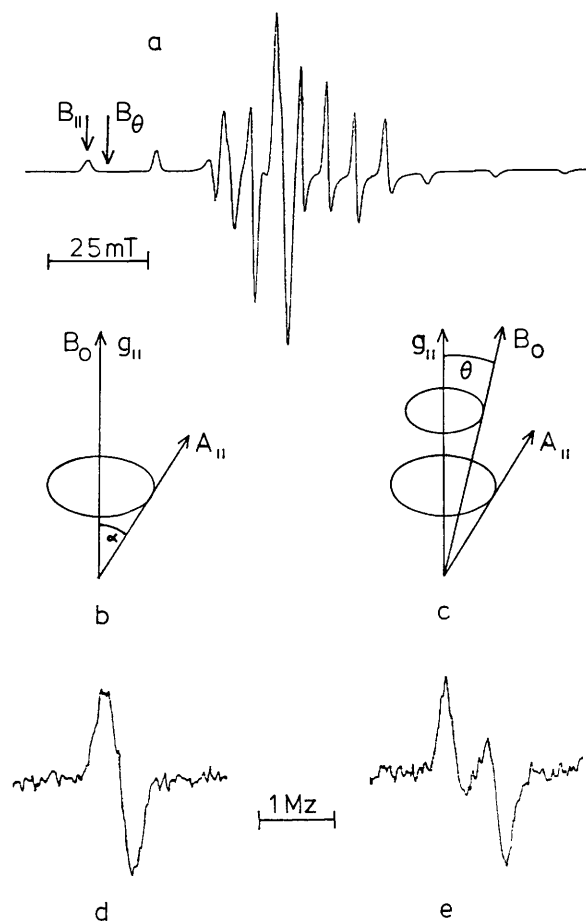
Figure 8 Orientation-selected ENDOR (a), Powder EPR of a vanadyl
complex, (b) and (c), orientation of the applied field with respect to
tensor axes for the points marked B and B_θ respectively, (d) and (e),
corresponding ENDOR spectra obtained from vanadyl-doped CsCl,
120 K A full commentary is given in the text

powder ENDOR signal, but from a limited range of orien-
tations An example is shown in Figure 8e, which was obtained
from vanadyl-doped CsCl for a setting of the field corresponding
to $\theta = 11°$

One could hope to be able to read directly from spectra like
that of Figure 8e the extrema in the ENDOR frequencies for the
particular value of θ and analysis of these as a function of θ
should enable A and α to be determined However, it is not
necessarily clear which points on the spectrum actually corres-
pond to the extrema in the ENDOR frequencies, so to optimize
the quality of the analysis it seems necessary to carry out
simulations It seems clear that, in general, the detailed shape of
the simulated spectra will depend on whether or not the orien-
tation dependence of the ENDOR transition moment is
included in the calculations The sensitivity of the calculated
spectra to the transition moment will depend on the particular
case, but preliminary calculations indicate that there are realistic
circumstances where the inclusion of the transition moment can
have a significant effect on the shapes of simulated spectra [26] It
would appear that there is scope for further investigation of this
matter

8 Conclusion

The role of the nuclear Zeeman energy in both well-established
and modern electron resonance experiments has been surveyed
In conclusion two further areas which may bear thinking about
will be mentioned

The first point concerns the Breit-Rabi levels When the
nuclear Zeeman energy is about half the effective hyperfine

splitting the low frequency ENCOR transiton lies at zero frequency, which implies an (avoided) crossing of Breit-Rabi levels The occurrence of such a crossing is exploited in muon level crossing experiments,[27] following up a suggestion due to Abragam [28] It remains to be seen whether interesting and useful effects, reflecting the magnetic field dependence of the nuclear Zeeman energy conventional electron resonance experiments

The final point is on the evolution of the magnetization of radical pairs and the polarization of their EPR spectra [29] Discussion of this for the case where the EPR spectra contain (M_I, M_I') transitions might be interesting and relevant to the behaviour of pairs in the solid state or, possibly, the slow motional regime

NOTE ADDED IN PROOF The comment about COSY made at the end of Section 6 has been overtaken, to some extent, by recent work (S Lee, B R Patyal, and J H Freed, *J Chem Phys*, 1993, **98**, 3665)

9 References

1 H M McConnell, C Heller, T Cole, and R W Fessenden, *J Am Chem Soc*, 1960, **82**, 766

2 N M Atherton and D H Whiffen, *Mol Phys*, 1960, **3** 1

3 I Miyagawa and W Gordy, *J Chem Phys*, 1960, **32**, 255

4 O Burghaus, E Haindl, M Plato, and K Mobius, *J Phys E Sci Instrum*, 1985, **18**, 294

5 Ya S Lebedev, in 'Modern Pulsed and Continuous Wave Electron Spin Resonance', ed L Kevan and M K Bowman, Wiley, New York, 1990, p 365

6 D E Budil, K A Earle, and J H Freed, in Advanced EPR Applications in Biology and Biochemistry', ed A J Hoff, Elsevier, Amsterdam, 1989, p 307

7 W Gordy, 'Theory and Applications of Electron Spin Resonance, Wiley, New York, 1980

8 N M Atherton, 'Principles of Electron Spin Resonance Ellis Horwood, Chichester, 1993

9 H M McConnell and J Strathdee, *Mol Phys*, 1959, **2**, 129

10 G T Trammell, H Zeldes, and R Livingston, *Phys Rev*, 1958, **110**, 630

11 W B Mims, *Phys Rev*, 1972, **B5**, 2409, 1972, **B6**, 3543

12 J Jeener, Ampere International Summer School, 1971, Basko Polje, Yugoslavia

13 R R Ernst, G Bodenhausen, and A Wokaun, 'Two Dimensional Nuclear Magnetic Resonance in Liquids', Oxford University Press, 1987

14 J Gorcester, G L Millhauser, and J H Freed, in 'Modern Pulsed and Continous Wave Electron Spin Resonance', ed L Kevan and M K Bowman, Wiley, New York, 1990, p 119

15 A Schweiger, *Angew Chem Int Ed Engl*, 1991, **30**, 265

16 see e g R K Harris, 'Nuclear Magnetic Resonance Spectroscopy', Longman, London, 1986

17 J Gorcester and J H Freed, *J Chem Phys*, 1988, **88**, 4678

18 J S Hyde, M D Smigel, L R Dalton, and L A Dalton, *J Chem Phys*, 1975, **62**, 1655

19 J Jeener, B H Meier, P Bachmann, and R R Ernst, *J Chem Phys*, 1979, **71**, 4546

20 see e g L R Dalton, B H Robinson, L A Dalton, and P Coffey, *Adv Magn Res*, 1976, **8**, 149

21 D Marsh and L Horvath, in 'Advanced EPR Applications in Biology and Biochemistry', ed A J Hoff, Elsevier, Amsterdam, 1989

22 see e g D H Whiffen, *Mol Phys*, 1966, **10**, 595, E R Davies and T Rs Reddy, *Phys Lett*, 1970, **31**, 398

23 B M Hoffman, R A Venters, and J Martinsen, *J Magn Res*, 1985, **62**, 537, T A Henderson, G C Hurst, and R W Kreilick, *J Am Chem Soc*, 1985, **107**, 7299, N D Yordanov and M Zdravkova, 1984, *Proc XXII Congr Ampere*, Zurich, p 612

24 G H Rist and J S Hyde, *J Chem Phys*, 1970, **52**, 4633

25 Electron Magnetic Resonance in Disordered Systems, ed N D Yordanov, World Scientific, Singapore, 1992

26 N M Atherton and C Oliva, unpublished work

27 S F J Cox, G H Eaton, J E Magraw, and C A Scott, *Chem Phys Lett*, 1989, **160**, 85

28 A Abragam, *Compt Rend Acad Sci (Paris)*, 1984, **299**, 95

29 see e g K A McLauchlan, in 'Modern Pulsed and Continuous Wave Electron Spin Resonance', ed L Kevan and M K Bowman, Wiley, New York, 1990, p 285